Method for driven-dissipative problems: Keldysh-Heisenberg equations

Yuanwei Zhang [1,*] and Gang Chen [2,3,4,†]

[1] *College of Physics and Electronic Engineering, Sichuan Normal University, Chengdu 610101, China*

[2] *State Key Laboratory of Quantum Optics and Quantum Optics Devices, Institute of Laser Spectroscopy, Shanxi University, Taiyuan, Shanxi 030006, China*

[3] *Collaborative Innovation Center of Extreme Optics, Shanxi University, Taiyuan, Shanxi 030006, China*

[4] *Collaborative Innovation Center of Light Manipulations and Applications, Shandong Normal University, Jinan 250358, China*

(Received 30 July 2020; accepted 20 November 2020; published 8 December 2020)

Driven-dissipative systems have recently attracted great attention due to the existence of novel physical phenomena with no analog in the equilibrium case. The Keldysh path-integral theory is a powerful tool to investigate these systems. However, it has still been a challenge to study strong nonlinear effects implemented by recent experiments, since in this case the photon number is few and quantum fluctuations play a crucial role in the dynamics of the system. Here we develop an approach for deriving exact steady states of driven-dissipative systems by introducing the Keldysh partition function in the Fock-state basis and then mapping the standard saddle-point equations into Keldysh-Heisenberg equations. We take the strong Kerr nonlinear resonators with and without the nonlinear driving as two examples to illustrate our method. It is found that, in the absence of the nonlinear driving, the exact steady state obtained does not exhibit bistability and agrees well with the complex P-representation solution. While in the presence of the nonlinear driving, the multiphoton resonance effects are revealed and are consistent with the qualitative analysis. Our method provides an intuitive way to explore a variety of driven-dissipative systems especially with strong correlations.

DOI: 10.1103/PhysRevA.102.062205

I. INTRODUCTION

In recent years, the driven-dissipative systems have gotten a lot of attention both theoretically and experimentally. In these systems, the nonlinear interactions can be significantly enhanced by controlling both the driving and dissipation processes. For example, strong optical nonlinearities at the single-photon level have already been observed in cavity quantum electrodynamics (QED) [1,2], Rydberg atomic systems [3–5], optomechanical systems [6], and superconducting circuit QED systems [7–12]. These advances in experimental methods have greatly promoted the development of quantum metrology, quantum information, and quantum optical devices [13,14]. On the other hand, they also provide good platforms for studying novel nonequilibrium physical phenomena, such as the dynamical critical phenomena [15–17], time crystals [18], and driven-dissipative strong correlations [19,20]. In this context, how to understand the nonlinear effects in nonequilibrium phenomena has become an important topic.

The Keldysh functional integral formalism in the coherent-state basis is a general approach to study nonequilibrium physics [21]. This technique provides a well-developed toolbox of perturbation techniques to study the nonlinear effects [22–24]. For example, in some systems such as the polariton condensates [15,16] and atomic ensembles in cavities [25–30], the single-particle actions are quadratic and the diagrammatic perturbation theory, based on Wick's theorem, can be performed. However, for coherently driven systems such as optomechanical systems [31–34], the single-particle actions are no longer quadratic and Wick's theorem cannot be applied directly. Fortunately, when the coherent driving is strong and the nonlinear interaction is weak, the mean photon number is large and the standard saddle-point approximation can be well introduced. In this approach, the mean values of operators are mainly determined by the classical path, which satisfies the saddle-point equations, and quantum fluctuations are treated as perturbations [22–24]. However, recent researches have focused on the strongly nonlinear effects at the level of individual photons, which are a benefit for processing quantum information [14]. Experimentally, these require the systems to be weakly driven and the nonlinear interactions to be strong. As a result, the mean photon number is few and quantum fluctuations play a crucial role in the dynamics of the system. This indicates that the standard saddle-point approximation is not reasonable.

To solve this crucial problem, we develop the Keldysh path-integral theory in the Fock-state basis, from which the standard saddle-point equations are mapped into quantum Hamiltonian equations named as Keldysh-Heisenberg equations. As a result, the exact steady states induced by the quantum fluctuation effect can be well derived. We take the strong Kerr nonlinear resonators with and without nonlinear driving as two examples to illustrate our method. It is found that, in the absence of the nonlinear driving, the exact steady state obtained does not exhibit bistability and agrees well with the complex P-representation solutions. While in the presence

*zywznl@163.com

†chengang971@163.com

of the nonlinear driving, the multiphoton resonance effects are revealed and are consistent with the qualitative analysis. Our method offers an effective way to explore a variety of driven-dissipative systems, especially with strongly correlated photons, based on the powerful toolbox of quantum field theory.

II. STANDARD SADDLE-POINT APPROXIMATION

We begin to consider a dissipative Kerr nonlinear resonator with a coherent driving term, in which the Hamiltonian is written as ($\hbar = 1$ hereafter)

$$\hat{H} = \Delta_c \hat{a}^\dagger \hat{a} + \chi \hat{a}^{\dagger 2} \hat{a}^2 + i\Omega(\hat{a}^\dagger - \hat{a}), \tag{1}$$

where $\hat{a}$ ($\hat{a}^\dagger$) is the annihilation (creation) operator of the resonator, $\Delta_c = \omega_c - \omega_p$ is the detuning with ω_c and ω_p being respectively the frequencies of the resonator and driving field, χ is the Kerr nonlinearity, and Ω is the driving amplitude. We assume that the resonator is coupled to a zero-temperature bath. Therefore, the dynamics of such a system are described by the Lindblad master equation [35,36]

$$\frac{d}{dt}\hat{\rho}(t) = \mathcal{L}\hat{\rho}(t) = -i[\hat{H}, \hat{\rho}(t)] + \gamma \mathcal{D}[\hat{a}]\hat{\rho}(t), \tag{2}$$

where $\hat{\rho}(t)$ is the density matrix, $\mathcal{L}$ is the Liouville superoperator, γ is the one-photon decay rate, and $\mathcal{D}[\hat{o}]\hat{\rho}(t) = \hat{o}\hat{\rho}(t)\hat{o}^\dagger - [\hat{o}^\dagger \hat{o}\hat{\rho}(t) + \hat{\rho}(t)\hat{o}^\dagger \hat{o}]/2$ is the standard dissipator in the Lindblad form. This Lindblad master equation can be investigated by the Keldysh nonequilibrium quantum field theory [22–24], in which the evolution takes place along the closed time contour.

We suppose $|\alpha\rangle$ as a coherent state, which is the eigenstate of the annihilation operator $\hat{a}$ with the complex eigenvalue a (i.e., $\hat{a}|\alpha\rangle = a|\alpha\rangle$). Note that the Keldysh close contour can be divided into a sequence of infinitesimal time steps, as shown in Fig. 1(a). Then the completeness relation in terms of the coherent state, $\hat{1}_{\rm coh} = \iint (da^* da/\pi) e^{-|a|^2} |\alpha\rangle\langle\alpha|$, is inserted in between consecutive time steps [24]. In this coherent-state basis, the partition function, which corresponds to the Lindblad master equation (2), is given by

$$Z = \int \mathfrak{D}[a_+, a_-] \exp(iS), \tag{3}$$

where $+$ and $-$ denote the forward and backward branches and the action

$$\begin{aligned} S = \int_{-\infty}^{+\infty} dt \Big\{ & a_+^*(i\partial_t - \Delta_c)a_+ - \chi a_+^{*2} a_+^2 - i\Omega(a_+^* - a_+) \\ & - a_-^*(i\partial_t - \Delta_c)a_- + \chi a_-^{*2} a_-^2 + i\Omega(a_-^* - a_-) \\ & - i\gamma a_+ a_-^* + i\frac{\gamma}{2}(a_+^* a_+ + a_-^* a_-) \Big\}. \end{aligned} \tag{4}$$

Note that the operators acting on the left- and right-hand sides of the density matrix in Eq. (2) are corresponding to the fields on the forward (+) and backward (−) time branches in the Keldysh formalism [24]. This leads to characteristics of the Keldysh functional integral with the doubling of degrees of freedom. Therefore, the time evolution can be interpreted as occurring along the closed Keldysh contour.

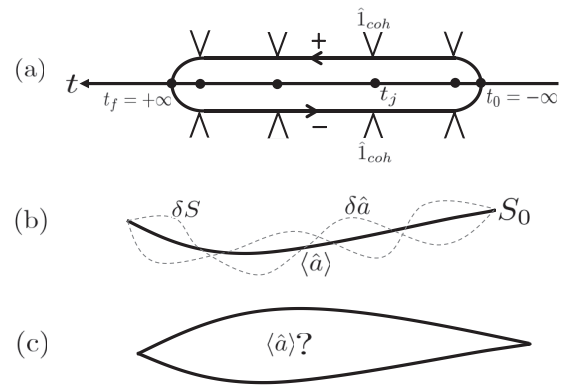

FIG. 1. (a) The Keldysh closed time contour in the coherent-state basis ($\hat{1}_{\rm coh}$). (b) Schematic diagram of the classical path (black solid line) and its quantum fluctuations (gray dashed lines). The classical path satisfies the saddle-point equations and has the action S_0, while the quantum fluctuations have the action δS. In the context of quantum optics, the operator $\hat{a}$ can be split into $\hat{a} \to \langle\hat{a}\rangle + \delta\hat{a}$, where $\langle\hat{a}\rangle$ describes the classical path, and $\delta\hat{a}$ governs the quantum fluctuation effect. (c) When the coherent driving is weak and the nonlinear interaction is strong, the saddle-point equations may have two solutions.

It is more convenient to discuss Eq. (4) in the Keldysh basis,

$$a_{cl} = \frac{1}{\sqrt{2}}(a_+ + a_-), \qquad a_q = \frac{1}{\sqrt{2}}(a_+ - a_-), \tag{5}$$

where a_{cl} and a_q are the classical and quantum fields [22–24]. After a straightforward calculation, the action is rewritten as

$$\begin{aligned} S = \int_{-\infty}^{+\infty} dt \Big\{ & a_{cl}^*(i\partial_t - \Delta_c)a_q + a_q^*(i\partial_t - \Delta_c)a_{cl} \\ & - i\frac{\gamma}{2}(a_{cl}^* a_q - a_{cl} a_q^*) + i\gamma a_q^* a_q - i\sqrt{2}\Omega(a_q^* - a_q) \\ & - \chi\left(a_{cl}^{*2} a_{cl} a_q + a_{cl} a_q^{*2} a_q + a_{cl}^* a_{cl}^2 a_q^* + a_{cl}^* a_q^* a_q^2\right) \Big\}. \end{aligned} \tag{6}$$

Note that in the presence of the coherent driving ($\Omega \neq 0$) the first two lines of Eq. (6) are not quadratic. Therefore, we cannot directly apply the diagrammatic perturbation theory, which is based on Wick's theorem, to calculate the nonlinear term. Fortunately, when the coherent driving is strong and the nonlinear interaction is weak, the mean photon number circulating inside the resonator is large and the light field behaves as a semiclassical field [35]. In such a case, the saddle-point approximation can be well used to investigate the dynamics of the system [22–24]. As show in Fig. 1(b), the mean values of operators are mainly determined by the classical path and quantum fluctuations are treated as perturbation. The classical path is determined by the principle of least action:

$$\frac{\delta S}{\delta a_{cl}^*} = 0, \quad \frac{\delta S}{\delta a_q^*} = 0, \tag{7}$$

which lead to two saddle-point equations

$$i\partial_t a_q = \tfrac{1}{2}(2\Delta_c + i\gamma)a_q + \chi\left(2a_{cl}^* a_{cl} a_q + a_{cl}^2 a_q^* + a_q^* a_q^2\right), \tag{8}$$

$$i\partial_t a_{cl} = i\sqrt{2}\Omega - i\gamma a_q + \tfrac{1}{2}(2\Delta_c - i\gamma)a_{cl}$$

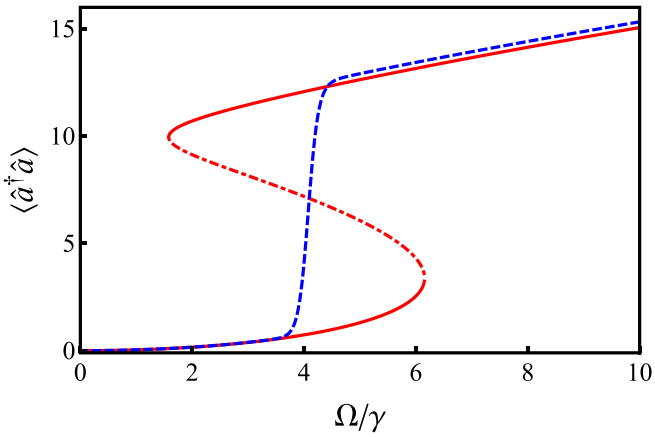

FIG. 2. The steady-state mean photon number $\langle \hat{a}^\dagger \hat{a} \rangle$ as a function of the coherent driving amplitude Ω/γ, when $\Delta_c/\gamma = 5$ and $\chi/\gamma = -0.25$. The red solid lines are the stable solutions of Eq. (11), while the red dash-dotted line is its unstable solution. These mean-field solutions reflect the optical bistability phenomenon. The blue dashed line is the exact steady-state solution from Eq. (26), which has considered the quantum fluctuation effect.

$$+\chi\left(2a_{cl}a_q^* a_q + a_{cl}^* a_{cl}^2 + a_{cl}^* a_q^2\right). \tag{9}$$

Equation (8) is always solved by

$$a_q = a_q^* = 0. \tag{10}$$

By substituting $a_q = a_q^* = 0$ into Eq. (6), we find the action $S = 0$ in the steady-state case. The more physical reason of these results is that in the steady state the action on the forward part of the contour is canceled by that on the backward part [22–24]. As a result, $S = 0$ and $a_+ = a_-$, i.e., $a_q = a_q^* = 0$. In addition, we also obtain $a_{cl} = \sqrt{2}a_0$, where $a_0 = a_+ = a_-$ is the steady-state mean value of $\hat{a}$, i.e., $a_0 = \langle \hat{a} \rangle$ [25]. By substituting $a_q = 0$ and $a_{cl} = \sqrt{2}a_0$ into Eq. (9) and making $i\partial_t a_{cl} = 0$, we obtain $a_0 = -2i\Omega/(2\Delta_c - i\gamma + 4\chi|a_0|^2)$, from which the mean photon number

$$\langle \hat{a}^\dagger \hat{a} \rangle = |a_0|^2 = \frac{4\Omega^2}{4(\Delta_c + 2\chi|a_0|^2)^2 + \gamma^2}. \tag{11}$$

This solution is identical to the mean-field solution of the steady state [35,36]. In fact, the saddle-point approximation is equivalent to the mean-field approach, named the linearization approximation, in quantum optics [35]. In the spirit of the linearization approximation, the operator $\hat{a}$ can be split into an average amplitude and a fluctuation term, i.e., $\hat{a} \to \langle \hat{a} \rangle + \delta\hat{a}$, where $\langle \hat{a} \rangle$ is determined by the mean-field equation. The correspondence between these two methods is shown in Fig. 1(b). As pointed out in Ref. [36], when the sign of Δ_c is opposite to that of χ, Eq. (11) may have two stable solutions (see the red lines of Fig. 2). In other words, the action of the system has two classical paths [see Fig. 1(c)]. As a result, the perturbation calculation around the classical path may be not reasonable. This phenomenon, called the optical bistability, signals the failure of both the linearization approximation and the saddle-point approximation. On the contrary, Drummond and Walls derived a complex P-representation solution for the steady state [36]. In that method, they considered the quantum fluctuation effect and found that the exact steady-state solution does not exhibit bistability.

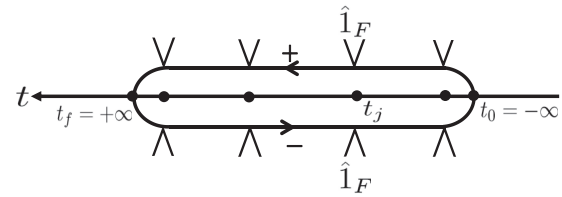

FIG. 3. The Keldysh closed time contour in the Fock-state basis ($\hat{1}_F = \sum_n |n\rangle\langle n|$).

III. KELDYSH-HEISENBERG EQUATIONS

We note that the standard saddle-point equations are based on the coherent-state basis. The coherent state is the closest quantum-mechanical state to a classical description of the field. It is a suitable representation for optical fields when the total photon number is large and quantum fluctuations are weak [35]. Obviously, this condition is not satisfied in the bistable region. As shown in Fig. 2, in that region the coherent driving is weak and the Kerr nonlinearity is the same order as the other parameters. Therefore, the mean photon number is not so large and quantum fluctuations induced by the Kerr nonlinearity cannot be ignored. To overcome this shortcoming, we introduce the Fock state, which is the eigenstate of the photon number operator. In the Fock-state basis, we develop a method using Keldysh-Heisenberg equations that governs the quantum fluctuation effect.

In the Fock-state basis, the completeness relation inserted in between consecutive time steps of the Keldysh close time contour becomes $\hat{1}_F = \sum_n |n\rangle\langle n|$ (see Fig. 3). In this case, the Keldysh partition function for stationary states reads (see Appendix A for details)

$$Z = \mathrm{Tr}[\exp(i\hat{S})], \tag{12}$$

where Tr denotes the trace operation which connects the two time branches, giving rise to the closed Keldysh contour [24]. $\hat{S}$ is the quantum action (like a time-evolution operator), where

$$\hat{S} = -\int_{-\infty}^{+\infty} \hat{\mathcal{H}}\, dt. \tag{13}$$

In Eq. (13), $\hat{\mathcal{H}}$ is a generalized Hamiltonian operator. As shown in Appendix A, $\hat{\mathcal{H}}$ consists of operators acting on different branches of the Keldysh closed time contour. For the driven-dissipative Kerr nonlinear resonator described in Eq. (2), the generalized Hamiltonian operator has the form

$$\begin{aligned}\hat{\mathcal{H}} = {} & \Delta_c \hat{a}_+^\dagger \hat{a}_+ + \chi \hat{a}_+^{\dagger 2}\hat{a}_+^2 + i\Omega(\hat{a}_+^\dagger - \hat{a}_+) \\ & -\Delta_c \hat{a}_-^\dagger \hat{a}_- - \chi \hat{a}_-^{\dagger 2}\hat{a}_-^2 - i\Omega(\hat{a}_-^\dagger - \hat{a}_-) \\ & +i\gamma \hat{a}_+ \hat{a}_-^\dagger - i\frac{\gamma}{2}(\hat{a}_+^\dagger \hat{a}_+ + \hat{a}_-^\dagger \hat{a}_-),\end{aligned} \tag{14}$$

where $\hat{a}_\pm$ ($\hat{a}_\pm^\dagger$) are the annihilation (creation) operators and the subscript $+$ ($-$) means that the operator only acts on the forward (backward) time branch. These operators obey the commutation relations: $[\hat{a}_+, \hat{a}_+^\dagger] = [\hat{a}_-, \hat{a}_-^\dagger] = 1$ and $[\hat{a}_+, \hat{a}_-] = 0$. Note that $\hat{\mathcal{H}}$ is a non-Hermitian operator and,

however, is fundamentally different from the usual one in quantum mechanics [37–39]. As we discussed above, the degrees of freedom are doubled in the Keldysh formalism. Therefore, the Hilbert space of $\hat{\mathcal{H}}$ is a doubling Hilbert space $\mathcal{H}_+ \otimes \mathcal{H}_-$, where $\mathcal{H}_+$ and $\mathcal{H}_-$ are the Hilbert spaces corresponding to $\hat{a}_+$ and $\hat{a}_-$, respectively. Comparing Eq. (13) with Eq. (4), it can be found that we only need to replace the complex variable a_+ (a_-) by the corresponding operator $\hat{a}_+$ ($\hat{a}_-$) and omit the derivative with respect to time.

The time evolution of $\hat{a}_\pm$ can be governed by (see Appendix B for details)

$$i\frac{d}{dt}\hat{a}_\pm = [\pm\hat{a}_\pm, \hat{\mathcal{H}}]. \tag{15}$$

We further define $\hat{a}_{cl} = (\hat{a}_+ + \hat{a}_-)/\sqrt{2}$ and $\hat{a}_q = (\hat{a}_+ - \hat{a}_-)/\sqrt{2}$ as the annihilation operators of the classical and quantum fields, respectively. Immediately, these operators obey the commutation relations: $[\hat{a}_{cl}, \hat{a}_{cl}^\dagger] = [\hat{a}_q, \hat{a}_q^\dagger] = 1$ and $[\hat{a}_q, \hat{a}_{cl}] = 0$. And the quantum action in Eq. (13) is changed to $\hat{S} = -\int_{-\infty}^{+\infty}\hat{\mathcal{H}}dt = -\int_{-\infty}^{+\infty}(\hat{\mathcal{H}}_\uparrow + \hat{\mathcal{H}}_\downarrow)dt$, where

$$\begin{aligned}\hat{\mathcal{H}}_\uparrow &= i\sqrt{2}\Omega\hat{a}_q^\dagger + \tfrac{1}{2}(2\Delta_c - i\gamma)\hat{a}_q^\dagger\hat{a}_{cl}\\ &\quad+\chi(\hat{a}_{cl}^\dagger\hat{a}_{cl} + \hat{a}_q^\dagger\hat{a}_q - 1)\hat{a}_q^\dagger\hat{a}_{cl},\end{aligned} \tag{16}$$

$$\begin{aligned}\hat{\mathcal{H}}_\downarrow &= -i\sqrt{2}\Omega\hat{a}_q - i\gamma\hat{a}_q^\dagger\hat{a}_q + \tfrac{1}{2}(2\Delta_c + i\gamma)\hat{a}_{cl}^\dagger\hat{a}_q\\ &\quad+\chi(\hat{a}_{cl}^\dagger\hat{a}_{cl} + \hat{a}_q^\dagger\hat{a}_q - 1)\hat{a}_{cl}^\dagger\hat{a}_q.\end{aligned} \tag{17}$$

Through these transformations, the Hilbert space of $\hat{\mathcal{H}}$ is changed to $\mathcal{H}_q \otimes \mathcal{H}_{cl}$, where $\mathcal{H}_q$ and $\mathcal{H}_{cl}$ are the Hilbert spaces corresponding to $\hat{a}_q$ and $\hat{a}_{cl}$, respectively. And the time evolutions of $\hat{a}_q$ and $\hat{a}_{cl}$ can be governed by the following equations:

$$\begin{aligned}i\frac{d}{dt}\hat{a}_q &= [\hat{a}_{cl}, \hat{\mathcal{H}}]\\ &= \frac{1}{2}(2\Delta_c + i\gamma)\hat{a}_q + \chi\left(2\hat{a}_{cl}^\dagger\hat{a}_{cl}\hat{a}_q + \hat{a}_{cl}^2\hat{a}_q^\dagger + \hat{a}_q^\dagger\hat{a}_q^2\right),\end{aligned} \tag{18}$$

$$\begin{aligned}i\frac{d}{dt}\hat{a}_{cl} &= [\hat{a}_q, \hat{\mathcal{H}}]\\ &= i\sqrt{2}\Omega - i\gamma\hat{a}_q + \frac{1}{2}(2\Delta_c - i\gamma)\hat{a}_{cl}\\ &\quad+\chi\left(2\hat{a}_{cl}\hat{a}_q^\dagger\hat{a}_q + \hat{a}_{cl}^\dagger\hat{a}_{cl}^2 + \hat{a}_{cl}^\dagger\hat{a}_q^2\right).\end{aligned} \tag{19}$$

Since Eqs. (18) and (19) are formally similar to the Heisenberg equations for an equilibrium system, we can call them Keldysh-Heisenberg equations. Interestingly, it is easy to verify that the Keldysh-Heisenberg equations can also be obtained by replacing a_{cl} and a_q in the saddle-point equations (8) and (9) with the corresponding operators. It means that the Keldysh-Heisenberg equations can also be obtained by quantizing the semiclassical saddle-point equations. In contrast to the standard saddle-point equations, Keldysh-Heisenberg equations can completely capture the information induced by quantum fluctuations. Therefore, we use them to obtain the exact steady-state solution.

We assume the steady-state wave function as $|\Psi_0\rangle$, which is a vector in the doubling Hilbert space $\mathcal{H}_q \otimes \mathcal{H}_{cl}$. Note that, in the steady state, the expectation values of operators do not evolve over time; i.e., $i\frac{d}{dt}\langle\Psi_0|\hat{a}_q|\Psi_0\rangle = 0$ and $i\frac{d}{dt}\langle\Psi_0|\hat{a}_{cl}|\Psi_0\rangle = 0$. Using these conditions and Eqs. (18) and (19), we obtain the following equations:

$$\begin{aligned}0 &= \langle\Psi_0|[\hat{a}_{cl}, \hat{\mathcal{H}}]|\Psi_0\rangle\\ &= \langle\Psi_0|\tfrac{1}{2}(2\Delta_c + i\gamma)\hat{a}_q\\ &\quad+\chi\left(2\hat{a}_{cl}^\dagger\hat{a}_{cl}\hat{a}_q + \hat{a}_{cl}^2\hat{a}_q^\dagger + \hat{a}_q^\dagger\hat{a}_q^2\right)|\Psi_0\rangle,\end{aligned} \tag{20}$$

$$\begin{aligned}0 &= \langle\Psi_0|[\hat{a}_q, \hat{\mathcal{H}}]|\Psi_0\rangle\\ &= \langle\Psi_0|i\sqrt{2}\Omega - i\gamma\hat{a}_q + \tfrac{1}{2}(2\Delta_c - i\gamma)\hat{a}_{cl}\\ &\quad+\chi\left(2\hat{a}_{cl}\hat{a}_q^\dagger\hat{a}_q + \hat{a}_{cl}^\dagger\hat{a}_{cl}^2 + \hat{a}_{cl}^\dagger\hat{a}_q^2\right)|\Psi_0\rangle.\end{aligned} \tag{21}$$

If $|\Psi_0\rangle$ is defined as a coherent state, i.e., $\hat{a}_q|\Psi_0\rangle = a_q|\Psi_0\rangle$ and $\hat{a}_{cl}|\Psi_0\rangle = a_{cl}|\Psi_0\rangle$, where a_q and a_{cl} are constants, we recover the mean-field saddle-point solutions by substituting a_q and a_{cl} into Eqs. (20) and (21), as discussed in Sec. II. However, these solutions cannot capture the information induced by quantum fluctuations and should be omitted. Instead, we find Eq. (20) can be solved by $\hat{a}_q|\Psi_0\rangle = 0$, i.e., $\hat{a}_+|\Psi_0\rangle = \hat{a}_-|\Psi_0\rangle$. As a result, the steady-state wave function can be assumed as

$$|\Psi_0\rangle = |0\rangle_q\sum_{m=0}^{+\infty}\beta_m|m\rangle_{cl}, \tag{22}$$

where $|m\rangle_{cl}$ is the Fock state in the occupation number basis and β_m is the expansion coefficient. Interestingly, using Eqs. (18) and (19) we find $|\Psi_0\rangle$ satisfies a generalized Schrödinger equation,

$$i\partial_t|\Psi_0\rangle = \hat{\mathcal{H}}|\Psi_0\rangle. \tag{23}$$

Substituting $\hat{\mathcal{H}}$ and the form of $|\Psi_0\rangle$ in Eq. (22) into the eigenequation $\hat{\mathcal{H}}|\Psi_0\rangle = h|\Psi_0\rangle$ where h is the eigenvalue, we find it can be fulfilled only for $h = 0$, i.e., $\hat{\mathcal{H}}|\Psi_0\rangle = 0$. Using $\hat{\mathcal{H}}|\Psi_0\rangle = 0$, it is also straightforward to verify $\langle\Psi_0|\hat{S}|\Psi_0\rangle = 0$. It means that the action on the forward part of the contour is canceled by that on the backward part. Therefore, the wave function in Eq. (22) is reasonable.

Using $\hat{\mathcal{H}}|\Psi_0\rangle = 0$ [or Eq. (21)], we can get a recursion relation for the expansion coefficient as

$$\beta_m = \sqrt{\frac{2}{m}}\frac{\epsilon}{x+m-1}\beta_{m-1}, \tag{24}$$

with $\epsilon = \Omega/(i\chi)$ and $x = (2\Delta_c - i\gamma)/(2\chi)$. Based on this recursion relation, the steady-state wave function

$$|\Psi_0\rangle = \frac{1}{\sqrt{N}}|0\rangle_q\sum_{m=0}^{+\infty}\frac{(\sqrt{2}\epsilon)^m}{\sqrt{m!}}\frac{\Gamma(x)}{\Gamma(x+m)}|m\rangle_{cl}, \tag{25}$$

where $\Gamma(x)$ is the gamma special function and $N = {}_0F_2(x^*, x; 2|\epsilon|^2)$ is the normalization constant with ${}_0F_2(x^*, x; 2|\epsilon|^2) = \sum_{m=0}^{+\infty}\frac{\Gamma(x^*)\Gamma(x)}{\Gamma(x^*+m)\Gamma(x+m)}\frac{(2|\epsilon|^2)^m}{m!}$ being the generalized hypergeometric function. According to the relation $\hat{a}_{cl} = (\hat{a}_+ + \hat{a}_-)/\sqrt{2}$, we obtain the steady-state correlation function

$$\begin{aligned}\langle\hat{a}^{\dagger l}\hat{a}^k\rangle &= \langle\hat{a}_-^{\dagger l}\hat{a}_+^k\rangle = \frac{1}{\sqrt{2^{l+k}}}\langle\Psi_0|\hat{a}_{cl}^{\dagger l}\hat{a}_{cl}^k|\Psi_0\rangle\\ &= \frac{(\epsilon^*)^l\epsilon^k\Gamma(x^*)\Gamma(x)}{\Gamma(x^*+l)\Gamma(x+k)}\frac{{}_0F_2(x^*+l, x+k; 2|\epsilon|^2)}{{}_0F_2(x^*, x; 2|\epsilon|^2)},\end{aligned} \tag{26}$$

which is equivalent to the complex P-representation solution in Ref. [36]. In Fig. 2, we plot the steady-state mean photon number $\langle\hat{a}^\dagger\hat{a}\rangle$ as a function of the coherent driving amplitude Ω. Obviously, the exact steady state does not exhibit bistability (see the blue dashed line).

IV. NONLINEAR DRIVING CASE

In this section, we extend our method to the two-photon nonlinear driving case implemented recently in superconducting quantum circuits [40]. The effective Hamiltonian reads

$$\hat{H}=\Delta_c\hat{a}^\dagger\hat{a}+\chi\hat{a}^{\dagger 2}\hat{a}^2+i\Omega(\hat{a}^\dagger-\hat{a})+\tfrac{1}{2}(\Lambda\hat{a}^{\dagger 2}+\Lambda^*\hat{a}^2), \quad (27)$$

where Λ is the complex amplitude of the two-photon driving term. The Lindblad master equation becomes

$$\frac{d}{dt}\hat{\rho}(t)=-i[\hat{H},\hat{\rho}(t)]+\gamma\mathcal{D}[\hat{a}]\hat{\rho}(t)+\kappa\mathcal{D}[\hat{a}^2]\hat{\rho}(t), \quad (28)$$

where κ is the two-photon loss rate.

In the presence of the two-photon driving and loss terms, we rewrite $\hat{\mathcal{H}}=\hat{\mathcal{H}}_\uparrow+\hat{\mathcal{H}}_\downarrow$ as

$$\begin{aligned}\hat{\mathcal{H}}_\uparrow=&\frac{1}{2}(2\Delta_c-i\gamma)\hat{a}_q^\dagger\hat{a}_{cl}+\chi(\hat{a}_{cl}^\dagger\hat{a}_{cl}+\hat{a}_q^\dagger\hat{a}_q-1)\hat{a}_q^\dagger\hat{a}_{cl}\\&+i\sqrt{2}\Omega\hat{a}_q^\dagger-i\frac{\kappa}{2}(\hat{a}_{cl}^\dagger\hat{a}_{cl}-\hat{a}_q^\dagger\hat{a}_q+1)\hat{a}_q^\dagger\hat{a}_{cl}\\&+\Lambda\hat{a}_q^\dagger\hat{a}_{cl}^\dagger,\end{aligned} \quad (29)$$

$$\begin{aligned}\hat{\mathcal{H}}_\downarrow=&\frac{1}{2}(2\Delta_c+i\gamma)\hat{a}_{cl}^\dagger\hat{a}_q+\chi(\hat{a}_{cl}^\dagger\hat{a}_{cl}+\hat{a}_q^\dagger\hat{a}_q-1)\hat{a}_{cl}^\dagger\hat{a}_q\\&-i\sqrt{2}\Omega\hat{a}_q+i\frac{\kappa}{2}(\hat{a}_{cl}^\dagger\hat{a}_{cl}-\hat{a}_q^\dagger\hat{a}_q+1)\hat{a}_{cl}^\dagger\hat{a}_q\\&-(i\gamma+2i\kappa\hat{a}_{cl}^\dagger\hat{a}_{cl})\hat{a}_q^\dagger\hat{a}_q+\Lambda^*\hat{a}_{cl}\hat{a}_q.\end{aligned} \quad (30)$$

Similar to the discussion in Sec. III, we formally define the steady-state wave function as $|\Psi_0\rangle$. Using the Keldysh-Heisenberg equations, we also find that $\hat{a}_q|\Psi_0\rangle=0$. Therefore, we can also define $|\Psi_0\rangle$ as $|\Psi_0\rangle=|0\rangle_q\sum_{m=0}^{\infty}\beta_m|m\rangle_{cl}$. It is also easy to verify that $\hat{\mathcal{H}}|\Psi_0\rangle=0$ and $\langle\Psi_0|\hat{\mathcal{S}}|\Psi_0\rangle=0$. Finally, using $\hat{\mathcal{H}}|\Psi_0\rangle=0$ we get a recursion relation for the expansion coefficient as

$$\begin{aligned}&[(2\Delta_c-i\gamma)+(2\chi-i\kappa)(m-1)]\sqrt{m}\beta_m\\&\quad=-i2\sqrt{2}\Omega\beta_{m-1}-2\Lambda\sqrt{m-1}\beta_{m-2}.\end{aligned} \quad (31)$$

The last term in Eq. (31), which corresponds to the term $\Lambda\hat{a}_q^\dagger\hat{a}_{cl}^\dagger$ in $\hat{\mathcal{H}}_\uparrow$, makes the recursion relation difficult to solve. To simplify the calculation, we use a displacement transformation $\hat{\mathcal{H}}'=e^{\lambda\hat{a}_{cl}^\dagger}(\hat{\mathcal{H}}_\uparrow+\hat{\mathcal{H}}_\downarrow)e^{-\lambda\hat{a}_{cl}^\dagger}=\hat{\mathcal{H}}'_\uparrow+\hat{\mathcal{H}}'_\downarrow$. Under this transformation, $\hat{a}_q$ is not changed ($e^{\lambda\hat{a}_{cl}^\dagger}\hat{a}_qe^{-\lambda\hat{a}_{cl}^\dagger}\to\hat{a}_q$), but $\hat{a}_{cl}$ has a displacement ($e^{\lambda\hat{a}_{cl}^\dagger}\hat{a}_{cl}e^{-\lambda\hat{a}_{cl}^\dagger}\to\hat{a}_{cl}-\lambda$). When choosing $\lambda=i\sqrt{2\Lambda/(2\chi-i\kappa)}$, the term $\Lambda\hat{a}_q^\dagger\hat{a}_{cl}^\dagger$ can be eliminated and the condition $\hat{\mathcal{H}}|\Psi_0\rangle=0$ is thus equivalent to $\hat{\mathcal{H}}'|\Phi_0\rangle=0$ with $|\Phi_0\rangle=e^{\lambda\hat{a}_{cl}^\dagger}|\Psi_0\rangle=|0\rangle_q\sum_{m=0}^{\infty}\phi_m|m\rangle_{cl}$, where ϕ_m is also the expansion coefficient. Since $\hat{\mathcal{H}}_\downarrow$ is proportional to $\hat{a}_q$, the equation $\hat{\mathcal{H}}'|\Phi_0\rangle=0$ reduces to $\hat{\mathcal{H}}'_\uparrow|\Phi_0\rangle=0$, where

$$\begin{aligned}\hat{\mathcal{H}}'_\uparrow=&\chi[\hat{a}_{cl}^\dagger\hat{a}_{cl}\hat{a}_{cl}-2\lambda\hat{a}_{cl}^\dagger\hat{a}_{cl}+(\hat{a}_{cl}-\lambda)(\hat{a}_q^\dagger\hat{a}_q-1)]\hat{a}_q^\dagger\\&-i\frac{\kappa}{2}[\hat{a}_{cl}^\dagger\hat{a}_{cl}\hat{a}_{cl}-2\lambda\hat{a}_{cl}^\dagger\hat{a}_{cl}-(\hat{a}_{cl}-\lambda)(\hat{a}_q^\dagger\hat{a}_q-1)]\hat{a}_q^\dagger\\&+i\sqrt{2}\Omega\hat{a}_q^\dagger+\tfrac{1}{2}(2\Delta_c-i\gamma)(\hat{a}_{cl}-\lambda)\hat{a}_q^\dagger.\end{aligned} \quad (32)$$

And the recursion relation for the expansion coefficient is given by

$$\phi_m=\frac{2\lambda}{\sqrt{m}}\frac{y+m-1}{z+m-1}\phi_{m-1}, \quad (33)$$

where $y=[-i2\sqrt{2}\Omega+\lambda(2\Delta_c-i\gamma)]/[2\lambda(2\chi-i\kappa)]$ and $z=(2\Delta_c-i\gamma)/(2\chi-i\kappa)$. This recursion relation is solved by $\phi_m=\frac{(2\lambda)^m}{\sqrt{m!}}\frac{\Gamma(y+m)}{\Gamma(z+m)}$, from which the steady-state wave function $|\Psi_0\rangle=e^{-\lambda\hat{a}_{cl}^\dagger}|\Phi_0\rangle$ is obtained by (see Appendix C for details)

$$|\Psi_0\rangle=\frac{1}{\sqrt{N}}|0\rangle_q\sum_{m=0}^{+\infty}(-\lambda)^m\frac{{}_2F_1(-m,y;z;2)}{\sqrt{m!}}|m\rangle_{cl}, \quad (34)$$

where $N=\sum_{m=0}^{+\infty}\frac{|\lambda|^{2m}}{m!}|{}_2F_1(-m,y;z;2)|^2$ is the normalization constant and ${}_2F_1(-m,y;z;2)=\sum_{n=0}^{+\infty}\frac{(-m)_n(y)_n}{(z)_n}\frac{2^n}{n!}$ is the generalized hypergeometric function with $(r)_n=\Gamma(r+n)/\Gamma(r)$. Based on Eq. (34), the steady-state correlation function is

$$\langle\hat{a}^{\dagger l}\hat{a}^k\rangle=\frac{1}{N\sqrt{2^{l+k}}}\sum_{m=0}^{+\infty}\frac{1}{m!}\mathcal{F}_{m+l}^*\mathcal{F}_{m+k}, \quad (35)$$

where $\mathcal{F}_{m+k}=(-\lambda)^{m+k}{}_2F_1[-(m+k),y;z;2]$. It can be verified that Eq. (35) is equivalent to the complex P-representation solution in Ref. [41].

Using Eq. (35), we can study the influence of different driving processes on the nonlinear effects. For example, we consider the multiphoton resonances in the weak driving regime, which are easy to observe in experiments and can be used to measure the photon-photon interactions [42]. In this situation, the mean photon number is small and the mean-field approach is not reasonable. We first make a qualitative prediction from the Hamiltonian (27). When the energy of n incident photons is equivalent to the energy of n photons inside the resonator, that is, $n\omega_p=n\omega_c+\chi n(n-1)$, the absorption of n pumping photons is favored. Expressed in terms of the detuning $\Delta_c=\omega_c-\omega_p$, this relation reads $\Delta_c/\chi=-(n-1)$. On the other hand, the parity of n depends on the driving processes. In the absence of the one-photon driving ($\Omega=0$ and $\Lambda\neq0$), an even number of pumping photons is favored (n is even) and $\Delta_c/\chi=-1,-3,-5,\ldots$, while in the presence of both the one- and two-photon driving ($\Omega\neq0$ and $\Lambda\neq0$), n can be any integer greater than 0 and $\Delta_c/\chi=0,-1,-2,-3,-4,\ldots$. In Fig. 4, we plot the steady-state mean photon number $\langle\hat{a}^\dagger\hat{a}\rangle$ as a function of the detuning Δ_c/χ, based on Eq. (35). This figure shows clearly that, in the absence of the one-photon pumping (see the blue dashed line), the photon resonances arise around $\Delta_c/\chi=-1$ and -3, while in the presence of both the one- and two-photon driving (see the red solid line), the photon resonances arise around $\Delta_c/\chi=0,-1,-2$, and -3. These results are consistent with the qualitative analysis.

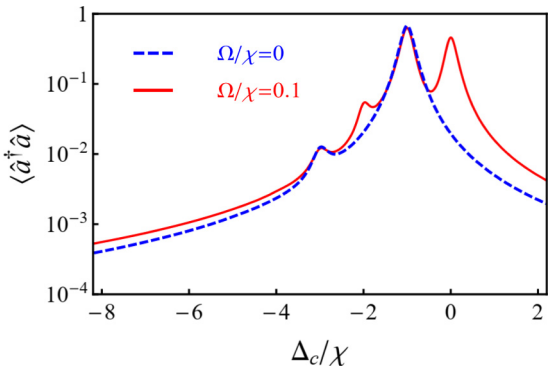

FIG. 4. The steady-state mean photon number $\langle\hat{a}^\dagger\hat{a}\rangle$ as a function of the detuning Δ_c/χ, when $\Omega/\chi = 0$ (blue dashed line) and $\Omega/\chi = 0.1$ (red solid line). The other parameters are chosen as $\gamma/\chi = 0.1$, $\kappa/\chi = 0.1$, and $\Lambda/\chi = 0.2$.

V. CONCLUSIONS

In summary, we have established the Keldysh path-integral theory in the Fock-state basis, from which the Keldysh-Heisenberg equations are successfully introduced. In contrast to the standard saddle-point equations, these quantum operator equations can well describe the quantum fluctuation effect and thus present the exact steady-state solutions. We have also considered two examples of the driven-dissipative Kerr nonlinear resonators with and without the two-photon nonlinear driving. Our results agree well with the qualitative analysis and those obtained by the complex P-representation method [36,41] and the coherent quantum-absorber method [43,44].

Before ending this paper, we compare our method with the complex P-representation method [36] and the coherent quantum-absorber method [43,44], both of which have also considered the quantum fluctuation effect. For the complex P-representation method, an operator master equation has been transformed to a c-number Fokker-Planck equation, and many complicated integration operations have to be faced. While for the coherent quantum-absorber method, an auxiliary resonator, which has the same Hilbert space dimension as the original resonator, should be introduced. By constructing the Hamiltonian for the auxiliary resonator appropriately, this cascaded system has a "dark" state. Then, one can get the steady state of the original system by tracing out the auxiliary cavity. Our developed Keldysh functional-integral method with the Keldysh-Heisenberg equations is more physical and intuitive. Moreover, it has the potential to deal with more complex problems, such as the nonequilibrium strong-correlated systems that have attracted much attention in both theory [17,45–48] and experiment [19,20]. However, the complex P-representation method and the coherent quantum-absorber method are not suitable for these problems. For the complex P-representation method, the form of c-number Fokker-Planck equation should satisfy the potential conditions. However, these conditions are usually not satisfied in the presence of interactions between different modes [35], whereas for the coherent quantum-absorber method, it is difficult to construct auxiliary resonators to simulate the coupling between strongly correlated systems and the environment. Instead, the Keldysh-Heisenberg equations could solve these complex problems since it can be easy to combine with powerful tools of quantum field theory, such as the linked-cluster expansion approach and the renormalization group method [22]. For example, we just need to divide the quantum action $\hat{S}$ as $\hat{S} = \hat{S}_0 + \hat{S}_I = -\int_{-\infty}^{+\infty}\hat{\mathcal{H}}_0 dt - \int_{-\infty}^{+\infty}\hat{\mathcal{H}}_I dt$, where $\hat{\mathcal{H}}_0$ is the solvable part of the generalized Hamiltonian $\hat{\mathcal{H}}$ and $\hat{\mathcal{H}}_I$ is the perturbation part. Then we can take the steady-state wave function of $\hat{\mathcal{H}}_0$ as the unperturbed steady state and calculate the influence of $\hat{\mathcal{H}}_I$ by the perturbation theory. We also noticed that in the previous literature of strong-correlated systems, the Keldysh path functional integral is in the coherent-state basis [17,46,47]. Therefore, the quantum fluctuation effects are still not been fully studied. In the near future, we hope our method can be extended to explore nonequilibrium phenomena induced by quantum fluctuations.

ACKNOWLEDGMENTS

This work is supported by the National Key R&D Program of China under Grant No. 2017YFA0304203, the National Natural Science Foundation of China under Grants No. 11674200, No. 11804241, and No. 12074232, and Shanxi "1331 Project" Key Subjects Construction.

APPENDIX A: KELDYSH PARTITION FUNCTION IN THE FOCK-STATE BASIS

In this Appendix, we derive the Keldysh partition function in the Fock-state basis in detail. A general Lindblad master equation reads

$$\frac{d}{dt}\hat{\rho}(t) = \mathcal{L}\hat{\rho}(t) = -i[\hat{H}, \hat{\rho}(t)] + \gamma\mathcal{D}[\hat{o}]\hat{\rho}(t), \tag{A1}$$

where $\hat{H}$ is any Hamiltonian of the system. For a one- or two-photon loss process, $\hat{o}$ can be chosen as $\hat{a}$ or $\hat{a}^2$. Without loss of generality, we set $\hat{o} = \hat{a}$ hereafter. Using the master equation (A1), the time evolution of the density matrix from t_0 to t_f is formally solved by

$$\hat{\rho}(t_f) = e^{(t_f - t_0)\mathcal{L}}\hat{\rho}(t_0) = \lim_{N\to\infty}(1 + \delta t\mathcal{L})^N\hat{\rho}(t_0), \tag{A2}$$

where we have decomposed the time evolution into a sequence of infinitesimal steps of duration $\delta t = (t_f - t_0)/N$. We focus on a single time step, and denote the density matrix after the jth step ($t_j = t_0 + j\delta t$) by $\hat{\rho}_j = \hat{\rho}(t_j)$. Then we have

$$\hat{\rho}_{j+1} = e^{\delta t\mathcal{L}}\hat{\rho}_j = (1 + \delta t\mathcal{L})\hat{\rho}_j + O(\delta t^2). \tag{A3}$$

Since the Liouville superoperator $\mathcal{L}$ acts on the density matrix "from both sides," it is more convenient to represent the density matrix in the Keldysh closed time contour. As shown in Fig. 3 of the main text, this can be achieved by projecting the density matrix into the two time branches [24]:

$$\hat{\rho}_j \equiv \hat{P}_{+,j}\hat{\rho}_j\hat{P}_{-,j}, \tag{A4}$$

where $\hat{P}_{+,j}$ ($\hat{P}_{-,j}$) is the projection operator on the forward (backward) branch at the time t_j. Obviously, if we choose $\hat{P}$ as a unit operator of the coherent state, i.e., $\hat{P} = \hat{1}_{\rm coh} = \iint(da^* da/\pi)e^{-|a|^2}|\alpha\rangle\langle\alpha|$, we can get the partition function in Sec. II [24]. Instead, here we choose $\hat{P}$ as the identity in the

Fock space, i.e., $\hat{P}_\pm = \hat{1}_F = \sum_n |n_\pm\rangle\langle n_\pm|$. In this case, $\hat{\rho}_j$ can be written as

$$\hat{\rho}_j \equiv \sum_{m,n} |m_+\rangle\langle m_+|\hat{\rho}_j|n_-\rangle\langle n_-| = \sum_{m,n} \langle m_+|\hat{\rho}_j|n_-\rangle|m_+\rangle\langle n_-|. \tag{A5}$$

We now consider $\hat{\rho}_{j+1} \equiv \sum_{k,l} \langle k_+|\hat{\rho}_{j+1}|l_-\rangle|k_+\rangle\langle l_-|$ in terms of the corresponding matrix element at the previous time step t_j. Inserting Eq. (A5) into Eq. (A3), we obtain

$$\begin{aligned}\langle k_+|\hat{\rho}_{j+1}|l_-\rangle &= \sum_{m,n} \langle k_+|[(1+\delta t\mathcal{L})(\langle m_+|\hat{\rho}_j|n_-\rangle|m_+\rangle\langle n_-|)]|l_-\rangle \\ &= \sum_{m,n} (\delta_{k,m}\delta_{l,n} - i\delta t\mathcal{H}_{k,l,m,n})\langle m_+|\hat{\rho}_j|n_-\rangle,\end{aligned} \tag{A6}$$

where

$$\begin{aligned}\mathcal{H}_{k,l,m,n} &= i\langle k_+|\mathcal{L}(|m_+\rangle\langle n_-|)|l_-\rangle \\ &= \langle k_+|\hat{H}|m_+\rangle\langle n_-|l_-\rangle - \langle k_+|m_+\rangle\langle n_-|\hat{H}|l_-\rangle \\ &\quad + i\gamma\langle k_+|\hat{a}|m_+\rangle\langle n_-|\hat{a}^\dagger|l_-\rangle \\ &\quad - i\frac{\gamma}{2}\langle k_+|\hat{a}^\dagger\hat{a}|m_+\rangle\langle n_-|l_-\rangle \\ &\quad - i\frac{\gamma}{2}\langle k_+|m_+\rangle\langle n_-|\hat{a}^\dagger\hat{a}|l_-\rangle.\end{aligned} \tag{A7}$$

Equation (A7) shows that the operators act on the forward or backward time branch, respectively. Therefore, we can introduce a generalized Hamiltonian operator:

$$\hat{\mathcal{H}} = \hat{H}_+ - \hat{H}_- + i\gamma\hat{a}_+\hat{a}_-^\dagger - i\frac{\gamma}{2}(\hat{a}_+^\dagger\hat{a}_+ + \hat{a}_-^\dagger\hat{a}_-), \tag{A8}$$

where $\hat{H}_\pm$ are the Hamiltonians of the forward and backward time branches, respectively. Based on Eqs. (A7) and (A8), $\mathcal{H}_{k,l,m,n}$ can be seen as a matrix element of $\hat{\mathcal{H}}$, i.e.,

$$\mathcal{H}_{k,l,m,n} = \langle n_-|\langle k_+|\hat{\mathcal{H}}|l_-\rangle|m_+\rangle, \tag{A9}$$

and the trace of $\hat{\rho}_{j+1}$ can thus be expressed as a simple form:

$$\begin{aligned}\mathrm{Tr}\hat{\rho}_{j+1} &= \mathrm{Tr}\sum_{k,l,m,n}(\delta_{k,m}\delta_{l,n} - i\delta t\mathcal{H}_{k,l,m,n})\langle m_+|\hat{\rho}_j|n_-\rangle|k_+\rangle\langle l_-| \\ &= \mathrm{Tr}\sum_{k,l,m,n}(\delta_{k,m}\delta_{l,n} - i\delta t\mathcal{H}_{k,l,m,n})|n_-\rangle|k_+\rangle\langle l_-|\langle m_+|\hat{\rho}_j \\ &= \mathrm{Tr}\big(1 - i\delta t\hat{\mathcal{H}}\big)\hat{\rho}_j \\ &= \mathrm{Tr}\big(e^{-i\delta t\hat{\mathcal{H}}}\hat{\rho}_j\big) + O(\delta t^2).\end{aligned} \tag{A10}$$

By iteration of Eq. (A10), the density matrix evolves from $\hat{\rho}(t_0)$ at t_0 to $\hat{\rho}(t_f)$ at $t_f = t_N$. This implies that in the limit $N \to \infty$ (and hence $\delta t \to 0$),

$$Z_{t_f,t_0} = \mathrm{Tr}\hat{\rho}(t_f) = \mathrm{Tr}[\exp(i\hat{S})\hat{\rho}(t_0)], \tag{A11}$$

with $\hat{S} = -\int_{t_0}^{t_f} \hat{\mathcal{H}}dt$.

Finally, we perform the limit, $t_0 \to -\infty$ and $t_f \to +\infty$, to get the Keldysh partition function for stationary states. Since in a Markov process, the initial state in the infinite past does not affect the stationary state [24], we can ignore the boundary term, i.e., $\hat{\rho}(t_0)$ in Eq. (A11), and obtain the final expression of the Keldysh partition function as

$$Z = \mathrm{Tr}[\exp(i\hat{S})], \tag{A12}$$

with the quantum action

$$\hat{S} = -\int_{-\infty}^{+\infty} \hat{\mathcal{H}}dt. \tag{A13}$$

APPENDIX B: DERIVING THE KELDYSH-HEISENBERG EQUATIONS

In this Appendix, we derive the Keldysh-Heisenberg equations by considering the average values of operators. For example, we define $\langle\hat{a}_+\rangle_j$ as the average value of $\hat{a}_+$ at time t_j. Using Eq. (A10), we find

$$\begin{aligned}\langle\hat{a}_+\rangle_{j+1} - \langle\hat{a}_+\rangle_j &= \mathrm{Tr}\hat{a}_+\hat{\rho}_{j+1} - \mathrm{Tr}\hat{a}_+\hat{\rho}_j \\ &= \mathrm{Tr}\sum_{k,l,m,n}(-i\delta t\mathcal{H}_{k,l,m,n})\langle m_+|\hat{\rho}_j|n_-\rangle\hat{a}_+|k_+\rangle\langle l_-| \\ &= \mathrm{Tr}\sum_{k,l,m,n}(-i\delta t\mathcal{H}_{k,l,m,n})|n_-\rangle(\hat{a}_+|k_+\rangle)\langle l_-|\langle m_+|\hat{\rho}_j \\ &= \mathrm{Tr}\sum_{k,l,m,n}(-i\delta t\mathcal{H}_{k,l,m,n})\hat{a}_+|n_-\rangle|k_+\rangle\langle l_-|\langle m_+|\hat{\rho}_j \\ &\quad + (i\delta t\mathcal{H}_{k,l,m,n})|n_-\rangle|k_+\rangle\langle l_-|\langle m_+|\hat{a}_+\hat{\rho}_j \\ &= \mathrm{Tr}\{-i\delta t[\hat{a}_+, \hat{\mathcal{H}}]\hat{\rho}_j\} \\ &= -i\delta t\langle[\hat{a}_+, \hat{\mathcal{H}}]\rangle_j\,.\end{aligned} \tag{B1}$$

Obviously, Eq. (B1) can be expressed as a simple form

$$i\frac{d}{dt}\langle\hat{a}_+\rangle = \langle[\hat{a}_+, \hat{\mathcal{H}}]\rangle. \tag{B2}$$

Similarly, we also find

$$\begin{aligned}\langle\hat{a}_-\rangle_{j+1} - \langle\hat{a}_-\rangle_j &= \mathrm{Tr}\hat{\rho}_{j+1}\hat{a}_- - \mathrm{Tr}\hat{\rho}_j\hat{a}_- \\ &= \mathrm{Tr}\sum_{k,l,m,n}(-i\delta t\mathcal{H}_{k,l,m,n})\langle m_+|\hat{\rho}_j|n_-\rangle|k_+\rangle\langle l_-|\hat{a}_- \\ &= \mathrm{Tr}\sum_{k,l,m,n}(-i\delta t\mathcal{H}_{k,l,m,n})|n_-\rangle|k_+\rangle(\langle l_-|\hat{a}_-)\langle m_+|\hat{\rho}_j \\ &= \mathrm{Tr}\sum_{k,l,m,n}(-i\delta t\mathcal{H}_{k,l,m,n})|n_-\rangle|k_+\rangle\langle l_-|\langle m_+|\hat{a}_-\hat{\rho}_j \\ &\quad + (i\delta t\mathcal{H}_{k,l,m,n})\hat{a}_-|n_-\rangle|k_+\rangle\langle l_-|\langle m_+|\hat{\rho}_j \\ &= \mathrm{Tr}\{-i\delta t[\hat{\mathcal{H}}, \hat{a}_-]\hat{\rho}_j\} \\ &= -i\delta t\langle[-\hat{a}_-, \hat{\mathcal{H}}]\rangle_j.\end{aligned} \tag{B3}$$

Thus, the dynamic equation of $\langle\hat{a}_-\rangle$ can be expressed as

$$i\frac{d}{dt}\langle\hat{a}_-\rangle = \langle[-\hat{a}_-, \hat{\mathcal{H}}]\rangle. \tag{B4}$$

Comparing with Eq. (B2), we find Eq. (B4) has a minus sign. The physical reason for this result is that $\hat{a}_-$ is on the backward time branch that has antitime ordering [22–24].

Therefore, the dynamics of $\hat{a}_+$ and $\hat{a}_-$ in the Heisenberg picture are described by

$$i\frac{d}{dt}\hat{a}_\pm = [\pm\hat{a}_\pm, \hat{\mathcal{H}}]. \tag{B5}$$

Finally, by defining $\hat{a}_{cl} = (\hat{a}_+ + \hat{a}_-)/\sqrt{2}$ and $\hat{a}_q = (\hat{a}_+ - \hat{a}_-)/\sqrt{2}$, we obtain the Keldysh-Heisenberg equations in the main text, i.e.,

$$i\frac{d}{dt}\hat{a}_q = [\hat{a}_{cl}, \hat{\mathcal{H}}], \quad i\frac{d}{dt}\hat{a}_{cl} = [\hat{a}_q, \hat{\mathcal{H}}]. \tag{B6}$$

APPENDIX C: STEADY-STATE WAVE FUNCTION FOR THE NONLINEAR DRIVING CASE

We present the detailed derivation of Eq. (34) of the main text. The steady-state wave function is

$$\begin{aligned}
|\Psi_0\rangle &= e^{-\lambda\hat{a}_{cl}^\dagger}|\Phi_0\rangle = \frac{1}{\sqrt{N}}e^{-\lambda\hat{a}_{cl}^\dagger}|0\rangle_q \sum_{k=0}^{+\infty}\phi_k|k\rangle_{cl} \\
&= \frac{1}{\sqrt{N}}|0\rangle_q \sum_{j=0}^{+\infty}\frac{(-\lambda\hat{a}_{cl}^\dagger)^j}{j!}\sum_{k=0}^{+\infty}\phi_k|k\rangle_{cl} \\
&= \frac{1}{\sqrt{N}}|0\rangle_q \sum_{j,k=0}^{+\infty}\frac{(-\lambda\hat{a}_{cl}^\dagger)^j}{j!}\frac{(2\lambda)^k}{\sqrt{k!}}\frac{(y)_k}{(z)_k}|k\rangle_{cl} \\
&= \frac{1}{\sqrt{N}}|0\rangle_q \sum_{j,k=0}^{+\infty}\frac{(2\lambda)^k(-\lambda)^j\sqrt{(j+k)!}}{j!k!} \\
&\quad\times\frac{(y)_k}{(z)_k}|j+k\rangle_{cl}.
\end{aligned} \tag{C1}$$

Letting $j + k = m$, we obtain

$$\begin{aligned}
|\Psi_0\rangle &= \frac{1}{\sqrt{N}}|0\rangle_q \sum_{m=0}^{+\infty}\sum_{k=0}^{m}\frac{(2\lambda)^k(-\lambda)^{m-k}m!}{\sqrt{m!}(m-j)!k!}\frac{(y)_k}{(z)_k}|m\rangle_{cl} \\
&= \frac{1}{\sqrt{N}}|0\rangle_q \sum_{m=0}^{+\infty}\sum_{k=0}^{m}\frac{(2\lambda)^k(-\lambda)^{m-k}m!}{\sqrt{m!}(m-j)!k!}\frac{(y)_k}{(z)_k}|m\rangle_{cl} \\
&= \frac{1}{\sqrt{N}}|0\rangle_q \sum_{m=0}^{+\infty}\sum_{k=0}^{m}\frac{2^k(-\lambda)^m(-1)^k m!}{\sqrt{m!}(m-j)!k!}\frac{(y)_k}{(z)_k}|m\rangle_{cl} \\
&= \frac{1}{\sqrt{N}}|0\rangle_q \sum_{m=0}^{+\infty}\sum_{k=0}^{+\infty}\frac{2^k(-\lambda)^m(-m)_k}{\sqrt{m!}k!}\frac{(y)_k}{(z)_k}|m\rangle_{cl} \\
&= \frac{1}{\sqrt{N}}|0\rangle_q \sum_{m=0}^{+\infty}(-\lambda)^m\frac{{}_2F_1(-m,y;z;2)}{\sqrt{m!}}|m\rangle_{cl}.
\end{aligned} \tag{C2}$$

[1] K. M. Birnbaum, A. Boca, R. Miller, A. D. Boozer, T. E. Northup, and H. J. Kimble, Photon blockade in an optical cavity with one trapped atom, Nature (London) **436**, 87 (2005).

[2] A. Reiserer, S. Ritter, and G. Rempe, Nondestructive detection of an optical photon, Science **342**, 1349 (2013).

[3] H. Gorniaczyk, C. Tresp, J. Schmidt, H. Fedder, and S. Hofferberth, Single-Photon Transistor Mediated by Interstate Rydberg Interactions, Phys. Rev. Lett. **113**, 053601 (2014).

[4] H. Busche, P. Huillery, S. W. Ball, T. Ilieva, M. P. A. Jones, and C. S. Adams, Contactless nonlinear optics mediated by long-range Rydberg interactions, Nat. Phys. **13**, 655 (2017).

[5] S. H. Cantu, A. V. Venkatramani, W. Xu, L. Zhou, B. Jelenković, M. D. Lukin, and V. Vuletić, Repulsive photons in a quantum nonlinear medium, Nat. Phys. **16**, 921 (2020).

[6] M. Aspelmeyer, T. J. Kippenberg, and F. Marquardt, Cavity optomechanics, Rev. Mod. Phys. **86**, 1391 (2014).

[7] P. Michler, A. Kiraz, C. Becher, W. V. Schoenfeld, P. M. Petroff, L. Zhang, E. Hu, and A. Imamoglu, A quantum dot single-photon turnstile device, Science **290**, 2282 (2000).

[8] A. Reinhard, T. Volz, M. Winger, A. Badolato, K. J. Hennessy, E. L. Hu, and A. Imamoğlu, Strongly correlated photons on a chip, Nat. Photonics **6**, 93 (2012).

[9] Z. Leghtas, S. Touzard, I. M. Pop, A. Kou, B. Vlastakis, A. Petrenko, K. M. Sliwa, A. Narla, S. Shankar, M. J. Hatridgeet *et al.*, Confining the state of light to a quantum manifold by engineered two-photon loss, Science **347**, 853 (2015).

[10] S. Touzard, A. Grimm, Z. Leghtas, S. O. Mundhada, P. Reinhold, C. Axline, M. Reagor, K. Chou, J. Blumoff, K. M. Sliwa *et al.*, Coherent Oscillations Inside a Quantum Manifold Stabilized by Dissipation, Phys. Rev. X **8**, 021005 (2018).

[11] A. Grimm, N. E. Frattini, S. Puri, S. O. Mundhada, S. Touzard, M. Mirrahimi, S. M. Girvin, S. Shankar, and M. H. Devoret, Stabilization and operation of a Kerr-cat qubit, Nature **584**, 205 (2020).

[12] R. Lescanne, M. Villiers, T. Peronnin, A. Sarlette, M. Delbecq, B. Huard, T. Kontos, M. Mirrahimi, and Z. Leghtas, Exponential suppression of bit-flips in a qubit encoded in an oscillator, Nat. Phys. **16**, 509 (2020).

[13] V. Giovannetti, S. Lloyd, and L. Maccone, Advances in quantum metrology, Nat. Photonics **5**, 222 (2011).

[14] A. Blais, S. M. Girvin, and W. D. Oliver, Quantum information processing and quantum optics with circuit quantum electrodynamics, Nat. Phys. **16**, 247 (2020).

[15] L. M. Sieberer, S. D. Huber, E. Altman, and S. Diehl, Dynamical Critical Phenomena in Driven-Dissipative Systems, Phys. Rev. Lett. **110**, 195301 (2013).

[16] L. M. Sieberer, S. D. Huber, E. Altman, and S. Diehl, Nonequilibrium functional renormalization for driven-dissipative Bose-Einstein condensation, Phys. Rev. B **89**, 134310 (2014).

[17] J. T. Young, A. V. Gorshkov, M. Foss-Feig, and M. F. Maghrebi, Non-Equilibrium Fixed Points of Coupled Ising Models, Phys. Rev. X **10**, 011039 (2020).

[18] F. M. Gambetta, F. Carollo, M. Marcuzzi, J. P. Garrahan, and I. Lesanovsky, Discrete Time Crystals in the Absence of Manifest Symmetries or Disorder in Open Quantum Systems, Phys. Rev. Lett. **122**, 015701 (2019).

[19] T. Tomita, S. Nakajima, I. Danshita, Y. Takasu, and Y. Takahashi, Observation of the Mott insulator to superfluid crossover of a driven-dissipative Bose-Hubbard system, Sci. Adv. **3**, e1701513 (2017).

[20] R. Ma, B. Saxberg, C. Owens, N. Leung, Y. Lu, J. Simon, and D. I. Schuster, A dissipatively stabilized Mott insulator of photons, Nature (London) **566**, 51 (2019).

[21] L. V. Keldysh, Diagram technique for nonequilibrium processes, Zh. Eksp. Teor. Fiz. **47**, 1515 (1964) [Sov. Phys. JETP **20**, 1018 (1965)].

[22] A. Altland and B. Simons, *Condensed Matter Field Theory* (Cambridge University Press, Cambridge, U.K., 2010).

[23] A. Kamenev, *Field Theory of Non-Equilibrium Systems* (Cambridge University Press, Cambridge, U.K., 2011).

[24] L. M. Sieberer, M. Buchhold, and S. Diehl, Keldysh field theory for driven open quantum systems, Rep. Prog. Phys. **79**, 096001 (2016).

[25] E. G. D. Torre, S. Diehl, M. D. Lukin, S. Sachdev, and P. Strack, Keldysh approach for nonequilibrium phase transitions in quantum optics: Beyond the Dicke model in optical cavities, Phys. Rev. A **87**, 023831 (2013).

[26] M. Buchhold, P. Strack, S. Sachdev, and S. Diehl, Dicke-model quantum spin and photon glass in optical cavities: Nonequilibrium theory and experimental signatures, Phys. Rev. A **87**, 063622 (2013).

[27] D. Nagy and P. Domokos, Nonequilibrium Quantum Criticality and Non-Markovian Environment: Critical Exponent of a Quantum Phase Transition, Phys. Rev. Lett. **115**, 043601 (2015).

[28] E. G. Dalla Torre, Y. Shchadilova, E. Y. Wilner, M. D. Lukin, and E. Demler, Dicke phase transition without total spin conservation, Phys. Rev. A **94**, 061802(R) (2016).

[29] Y. Shchadilova, M. M. Roses, E. G. Dalla Torre, M. D. Lukin, and E. Demler, Fermionic formalism for driven-dissipative multilevel systems, Phys. Rev. A **101**, 013817 (2020).

[30] P. Kirton, M. M. Roses, J. Keeling, and E. G. Dalla Torre, Introduction to the Dicke model: From equilibrium to nonequilibrium, and vice versa, Adv. Quantum Technol. **2**, 1800043 (2019).

[31] M.-A. Lemonde, N. Didier, and A. A. Clerk, Nonlinear Interaction Effects in a Strongly Driven Optomechanical Cavity, Phys. Rev. Lett. **111**, 053602 (2013).

[32] M.-A. Lemonde and A. A. Clerk, Real photons from vacuum fluctuations in optomechanics: The role of polariton interactions, Phys. Rev. A **91**, 033836 (2015).

[33] M.-A. Lemonde, N. Didier, and A. A. Clerk, Enhanced nonlinear interactions in quantum optomechanics via mechanical amplification, Nat. Commun. **7**, 11338 (2016).

[34] Y. Zhang, Quadratic optomechanical coupling in an active-passive-cavity system, Phys. Rev. A **101**, 023842 (2020).

[35] D. F. Walls and G. J. Milburn, *Quantum Optics* (Springer, New York, 2008).

[36] P. D. Drummond and D. F. Walls, Quantum theory of optical bistability. I. Nonlinear polarisability model, J. Phys. A **13**, 725 (1980).

[37] C. M. Bender and S. Boettcher, Real Spectra in Non-Hermitian Hamiltonians having $\mathcal{PT}$ Symmetry, Phys. Rev. Lett. **80**, 5243 (1998).

[38] C. M. Bender, Making sense of non-Hermitian Hamiltonians, Rep. Prog. Phys. **70**, 947 (2007).

[39] C. E. Rüer, K. G. Makris, R. El-Ganainy, D. N. Christodoulides, M. Segev, and D. Kip, Observation of parity-time symmetry in optics, Nat. Phys. **6**, 192 (2010).

[40] V. V. Sivak, N. E. Frattini, V. R. Joshi, A. Lingenfelter, S. Shankar, and M. H. Devoret, Kerr-Free Three-Wave Mixing in Superconducting Quantum Circuits, Phys. Rev. Appl. **11**, 054060 (2019).

[41] N. Bartolo, F. Minganti, W. Casteels, and C. Ciuti, Exact steady state of a Kerr resonator with one- and two-photon driving and dissipation: Controllable Wigner function multimodality and dissipative phase transitions, Phys. Rev. A **94**, 033841 (2016).

[42] M. A. Macovei, Measuring photon-photon interactions via photon detection, Phys. Rev. A **82**, 063815 (2010).

[43] K. Stannigel, P. Rabl, and P. Zoller, Driven-dissipative preparation of entangled states in cascaded quantum optical networks, New J. Phys. **14**, 063014 (2012).

[44] D. Roberts and A. A. Clerk, Driven-Dissipative Quantum Kerr Resonators: New Exact Solutions, Photon Blockade and Quantum Bistability, Phys. Rev. X **10**, 021022 (2020).

[45] Y. Ashida, S. Furukawa, and M. Ueda, Quantum critical behavior influenced by measurement backaction in ultracold gases, Phys. Rev. A **94**, 053615 (2016).

[46] M. F. Maghrebi, Fragile fate of driven-dissipative XY phase in two dimensions, Phys. Rev. B **96**, 174304 (2017).

[47] T. Graß, Excitations and correlations in the driven-dissipative Bose-Hubbard model, Phys. Rev. A **99**, 043607 (2019).

[48] M. Nakagawa, N. Tsuji, N. Kawakami, and M. Ueda, Dynamical Sign Reversal of Magnetic Correlations in Dissipative Hubbard Models, Phys. Rev. Lett. **124**, 147203 (2020).